Egyptian Journal of Medical Microbiology Volume 29 / No.4 / October 2020 35-44 Online ISSN: 2537-0979

ORIGINAL ARTICLE

Assessment of Therapeutic Efficacy of Mesenchymal Stem Cells in Doxorubicin- Induced Skeletal Myopathy: A histological and Immunological Experimental Study

[1]Ahmed H. Bayoumi, [2]Ahmed El Zainy, [3]Amul M. Badr, [4]Dina Fawzy, [5]Amal A. Elshimy*

[1]Department of Anatomy and Embryology, Faculty of Medicine, Cairo University, Cairo, Egypt
[2]Department of Anatomy and Histology, College of Medicine, Qassim University, Qassim, Saudi Arabia and Department of Anatomy and Embryology, College of Medicine, Cairo University, Cairo, Egypt
[3]Department of Biochemistry, Faculty of Medicine, Cairo University, Cairo, Egypt
[4]Department of Pathology, Faculty of Medicine, Cairo University, Cairo, Egypt
[5]Department of Medical Microbiology and Immunology, Faculty of Medicine, Cairo University, New Giza University, Cairo, Egypt

Key words:
Doxorubicin, Bone Marrow Mesenchymal stem cells (BMMSCs), Tumour necrosis factor-alpha (TNF-α), albino rat, skeletal muscle.

Corresponding Author:
Amal Ali Elshimy
Department of Medical Microbiology and Immunology, Faculty of Medicine, Cairo University, New Giza University,
Tel.: +201019656753
aelshimy@ngu.edu.eg

ABSTRACT

Background*: Doxorubicin is an effective chemotherapeutic drug that commonly induce pathological alteration in skeletal muscles. Bone- marrow mesenchymal stem cells (BMMSCs) offer a therapeutic potential for tissue repair and regeneration. Tumour necrosis factor-alpha (TNF-α) and Interleukin-1 beta (IL-1β) display worthy biomarkers for tissue damage and repair.* ***Objectives****: The aim of the current study was to evaluate the therapeutic effect of BMMSCs on doxorubicin - induced skeletal myopathy in experimental animals, through histological studies, antioxidant activity and investigation of TNF-α, IL-1β as diagnostic parameters for muscle damage and regeneration.* ***Methodology:*** *40 adult albino-rats were divided into 4 equal groups; Group-I (control group) injected with phosphate-buffered saline (PBS), Group-II: doxorubicin- induced myopathy model group; received no treatment, Group-III: doxorubicin- induced myopathy model left for spontaneous muscle recovery, and Group-IV: doxorubicin-induced myopathy treated with systemic BMMSCs. The skeletal muscle regeneration evaluated through histological and antioxidant activity studies and investigation of TNF-α, IL-1β and vascular endothelial growth factor (VEGF) levels.* ***Results:*** *Photomicrographic studies of the muscle fibers showed a more evident regeneration in MSCs treated groups (IV) when compared with the other groups received no treatment. A significant reduced levels of TNF-α, IL-1β, and increased both VEGF and antioxidant activity were demonstrated in group IV when compared with the other groups received no treatment.* ***Conclusion:*** MSCs is a promising therapy for doxorubicin-induced skeletal myopathy. TNF-α, and IL-1β are helpful biomarkers for evaluation of SCs therapeutic efficacy.

INTRODUCTION

Doxorubicin represents one of the most successful anti-tumor chemotherapeutics. It is used in treatment of many types of cancer [1]. Doxorubicin (adriamycin) is antibiotic anti-tumor which was first isolated from the Streptomyces peucetius bacterium in 1967 [2, 3].

Doxorubicin has many adverse effects on different body organs including muscle pain, weakness and myotoxicity. Doxorubicin - myotoxicity is mediated by mitochondrial, DNA, and oxidative damage of skeletal muscles fibers [4, 5].

One of the contributing mechanisms to doxorubicin-myotoxicity is the induction of excess levels of TNF-α which causes contractile dysfunction [6, 7]. TNF-α levels are high in patients with cancer; doxorubicin treatment exacerbates this rise in TNF levels [8]. Animals treated with doxorubicin demonstrated a similar elevation in TNF levels[9]. Therefore, TNF-α may display a biomarker for diagnosis and evaluation of possible therapeutic lines for doxorubicin- induced skeletal myopathy [7].

BMMSCs are pluripotent cells that can induce tissue regeneration and repair through its ability to differentiate into many types of cells. BMMSCs among the most studied, and promising types of cells for treatment of many diseases[10,11,12].

Spontaneous skeletal muscle fibres recovery is very limited due to defective mitosis and poor regeneration[13]. Through their myogenic potential and anti-inflammatory and antioxidant capability; MSCs

DOI : https://doi.org/10.51429/EJMM29405

represents a superior choice when compared with myoblasts in skeletal muscle transplantation[12,14,15].

Management trials with biomarkers extensively needed to clarify the pathogenesis and evaluate possible therapeutic options for doxorubicin- induced skeletal myopathy. Therefore, the current study was conducted to investigate the therapeutic effect of BMMSCs and the diagnostic value of TNF-α and IL-1β in doxorubicin-induced skeletal myopathy.

METHODOLOGY

Doxorubicin (Adriamycin):

Adriamycin was purchased as vials from Phramacia Italia U.S.P Italy.

Isolation, culture and labeling of MSCs:

MSCs obtained from the research laboratory at the Biochemistry and Molecular Biology Unit, Faculty of Medicine, Cairo University. Bone marrow stromal cells were aspirated from albino rats femur and tibia. They were attained by flushing the bone marrow cavity with Dulbecco's Modified Eagle's Medium (DMEM) (Sigma, USA, D5796) with 10% fetal bovine serum (FBS) (Sigma, USA, F6178). The cells were spread over Ficoll-Hypaque (Sigma, USA, F8016) in a 2:1 ratio in a sterile conical tube and then centrifuged. The opaque mononuclear cell layer was then aspirated and inoculated into 1% Penicillin-Streptomycin supplemented culture medium (Sigma, USA, P4333) then incubated at 37°C for 14 days. When confluent colonies appeared (80-90%), cultures were rinsed twice with phosphate buffer saline (PBS) (Sigma, USA, P5493) and cells were treated with trypsin (0.25%) (Sigma, USA, T1426) for 5 minutes at 37°C in 1ml Ethylene Diamine Tetra Acetate (EDTA) (Sigma, USA, E6758) then centrifuged at 2400 rpm for 20 minutes. The resultant cell pellets were re-suspended in serum-supplemented medium and incubated in 25cm^2 culture flasks. The resultant cultures referred to as first passage cultures [16].

MSC in culture were characterized by their fusiform shape, adhesiveness, and demonstration of CD29 [17].

Labeling of MSCs with PKH26 dye and cell viability testing:

Cell Culture were labeled with cell tracker PKH26; a red fluorescent dye (Sigma Aldrich, USA, MINI26) according to manufacturer's instructions [18]. Cell viability was detected by adding 1:1 ratio of 0.4 % trypan blue stain, and cell suspension [19]. The cells were examined using fluorescence microscopy (Sigma-Aldrich, Saint Louis, USA). Detection of MSCs labelled with PKH26 fluorescent dye in the hepatic tissue was done one week after administration, and confirmed homing of these cells into the skeletal muscle tissue [20] (Fig. 1).

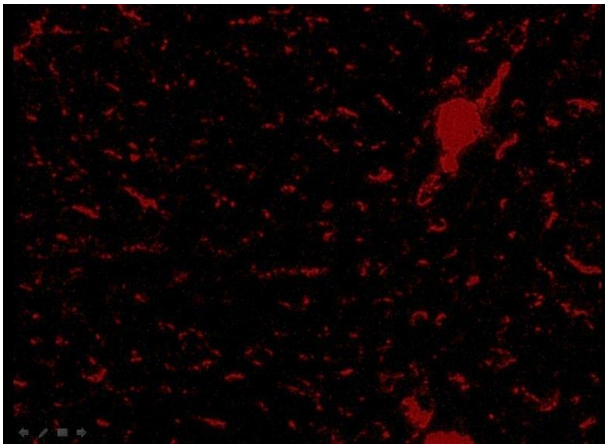

Fig. 1: Photomicrograph of a section of a rat skeletal muscle showing red fluorescent labelled MSCs with PKH26 dye in group IV (PKH x200).

Animals and Experimental Design:

Forty male *Sprague Dawley* (SD) adult albino rats weight 180±40 gram were used in this study. They were purchased from the Animal Facility, at Faculty of Medicine, Cairo University, Egypt. Animals were locally bred at standard room temperature (18-22˚C) fed free and maintained under standard conditions in accordance with the international guidelines for use of laboratory animals[18]. The experiment protocol including animal treatment, and anesthesia was approved by the Ethics Committee, Faculty of Medicine, Cairo University. The included forty SD rats in the present study were divided into 4 equal groups; 10 rats each.

Group I (control group)*:*

Ten SD rats received 1 ml PBS (0.9%) by intra-peritoneal injection on day 14, 21, 28 and 35.

Group II (doxorubicin- induced myopathy model group, with no treatment):

Ten SD rats of this group received an intra-peritoneal injection of doxorubicin in normal saline (3.750 mg/kg) on day 14, 21, 28 and 35 to reach a cumulative dose of 15 mg/kg. Rats of this group were sacrificed on the following day of the last dose of doxorubicin administration.

Group III (Doxorubicin induced myopathy model group, with spontaneous recovery):

Ten SD rats of this group received an intra-peritoneal injection of doxorubicin in normal saline (3.750 mg/kg) on day 14, 21, 28 and 35 to reach a cumulative dose of 15 mg/kg. Rats of this group were sacrificed 30 days after the last dose of doxorubicin administration [19].

Group IV (BMMCS treated group):

Ten rats of this group were injected with doxorubicin in normal saline at a dose of (3.750 mg/kg) on day 14, 21, 28 and 35 to reach a cumulative dose of (15 mg/kg).Each rat received one systemic injection of MSCs (1x10^6) diluted in 1 ml of phosphate buffer

saline, through the tail vein, one day after the last dose of doxorubicin injection. Rats of this group were sacrificed 30 days after SCs administration[20].

By the end of the experiment, the animals were sacrificed and the skeletal muscles were dissected for the following investigations**:**

Quantitative real-time polymerase reaction (RT-PCR): Measurement of TNF-α and IL-1β genes expression

The broilers' muscle specimens were studied for detection of mRNA concentrations of TNF-α, andIL-1β by quantitative real-time PCR. β- actin gene expression was used as a house keeping gene to normalize the gene expression data.

The primers used for TNF-α were:

- forward: 5′ -CCCCGACTACGTGCTCCTC-3′ and
- reverse: 5′ -GAACGGATGAACACGCCAGTC-3′

The primers used for IL-1β were:

- forward: 5′-CAAGGA GAGACAAGCAACGACAA-3′ and
- reverse: 5′ -GTCCCGACCATTGCTGTTTC-3′

All the gene primers were designed by using the chicken sequences from GenBank. Total RNA was attained by TRIzol reagent (Invitrogen, Carlsbad, CA, USA) following the manufacturer's instructions, and the RNA integrity was investigated by 1% agarose gel electrophoresis. The RNA levels were measured by OD260/280 readings (ratio >1.8) using a NanoDrop ND-1000 spectrophotometer (Nano-Drop Technology, Washington, DE).The RNA was reverse transcribed to cDNA by use of a PrimeScript RT reagent kit (Takara, Shiga, Japan). Real-time quantitative PCR was carried out in a 7500 Real-Time PCR system (Biosystem, Foster City, CA, USA) using a SYBR Green PCR-kit (Roche Diagnostics, Laval, Quebec, Canada). All samples were studied in triplicate, and the results were expressed as $2-\Delta\Delta CT$. Each cycle included denaturation at 95◦C for 10 seconds, annealing at 95◦C for 5 seconds, and extension at 60◦C for 34 seconds. Values normalized to the beta- actin gene. The relative quantification was measured by the expression $2^{-\Delta\Delta Ct}$ and calculated as fold change of the background level measured in group I (control group) [23].

***Measurement of VEGF genes by quantitative RT-PCR*[24]**

Total RNA was isolated by RNeasy Mini Kit (Qiagen, Valencia, CA). Reverse transcription was performed using AMV transcriptase (Promega, Madison, WI) to amplify the first cDNA strand from 2 µg of RNA. cDNA strands were further amplified with platinum *pfx* polymerase (Invitrogen, Carlsbad, CA). The RT-PCR of β-actin was used as an internal control.

The primers used for VEGF were:

Forward:

5′-CCC AAG CTT GAA ACC ATG AAC TTG CT-3′ and Backward:

5′-GCTCTA GAT CAT TCA TTC ACC GCC T-3′

The primers used for β-actin were:

Forward:

5′-TGG AAT CCT GTGGCA TCC ATG AAA-3′ and Backward:

5′-TAA AAC GCA GCT CAG TAA CAGTCC G-3′

Each cycle included denaturation at 45 °C for 45 minutes, 94 °C for 3 minutes, 20 cycles at 94 °C for 30 seconds, 58 °C for 30 seconds, and 72 °C for 1 minute. The PCR products were separated on 0.8 % agarose gel electrophoresis for 30 minutes.

Light microscopy study:

Haematoxylin and eosin stain

Muscle tissues were fixed in 4% formaldehyde. The sections were processed and stained according to *Kiernan* [25], four micron sections were examined.

Masson's trichrome stain

It was carried out according to *Clavi et al.* [26].

Electron microscopy study:

Small cylinders (4 mm long x×1 mm x1 mm) of tissue were prepared from each equatorial muscle section. These muscle tissue were then fixed by immersion in vials with 1 mL of glutaraldehyde (1.25%) and paraformaldehyde (1%) in PBS, at 4°C for 48 h. The sections were then studied and photographed by Joel, 100 CX II Transmission electron microscope (Jeol, Tokyo, Japan). Images taken by CCD camera model AMT according to *Hayat 2000* [27].

***Collagen area percent study*:**

Collagen area percent was studied by digital photographs of the Masson's trichrome stained slides that taken at 20× and 400× magnification using an inverted-light microscope (Nikon Eclipse TS100, Nikon Digital Sight DS-Fi1 mounted-digital camera). Images were analyzed using Image J software12. The software used to outline the area of interest, counted in pixels and then converted to metric units (Image J software12) [28].

Antioxidant Enzymes:

Superoxide dismutase (SOD) activity was studied using adrenaline auto-oxidation inhibition testing, with absorbance rate at 480 nm. Catalase activity was measured through the hydrogen peroxide reduced levels at 240 nm and the results were expressed as U/total protein mg. Enzyme activity results were investigated by spectrophotometer (Biomate 3S, Thermo Scientific—Waltham, MA, USA), using the Bradford assay [29, 30].

Statistical analysis:

The collected data were organized, tabulated and statistically analyzed using SPSS software statistical computer package version 22 (SPSS Inc, USA). The mean and standard deviation (SD) were calculated. One way ANOVA (Analysis of variance) was used to test the difference about mean values of measured variables among groups, multiple comparison between pairs of groups were performed using Tukey HSD (Post hoc range test). For interpretation of results of tests of significance, significance was adopted at $P \leq 0.05$ [31].

RESULTS

QRT-PCR for TNF-α and IL-1β:

TNF-α, and IL-1β levels were significantly higher in group II, and III when compared with group I (control group) and group IV. No significant differences in both TNF-α and IL-1β among group I and IV which demonstrated the therapeutic effect of MSCs on muscle regeneration. However, expression of both TNF-α and IL1β did not display significant variation between group II, and III which implicated weak muscle spontaneous regeneration (Table1).

Table 1: QRT- PCR products of TNF-α and IL1β in skeletal muscle tissue of the examined animals (mean ± SD).

	Group I	Group II	Group III	Group IV
TNF-α	2.81±0.58	8.72±1.1*	6.72±1.71*	3.9±1.37
IL-1β	1.22±0.24	6.53±1.61*	5.65±1.76*	2.58±0.69

*Significant P < 0.05

QRT-PCR of VEGF:

Expression of VEGF was significantly higher in group IV when compared with group I (control group). However, a significantly higher levels of VEGF were detected in groups III and IV when compared to group II. Although the difference between VEGF expression in groups III and IV was statistically significant, which implicated the superior regenerative activity of MSCs over the spontaneous muscle recovery (Table 2).

Table 2: QRT- PCR products of VEGF in muscle tissue of the examined animals (mean ± SD).

	Group I	Group II	Group III	Group IV
VEGF	2.2 ± 0.7	1.8 ± 0.24*	3.71± 1.13*	7.45 ± 1.63*

*Significant P < 0.05

Histological results:

Light microscopy haematoxylin and eosin stain results:

- Group I (Normal control); skeletal muscle specimens examination showed normal architecture of skeletal muscle, parallel muscle fibres with acidophilic striated sarcoplasm peripheral oval vesicular nuclei. Loose connective tissue endomysium separating the muscle fibres that featured a small blood vessel (Fig. 2 a).
- Group II showed degenerated pale acidophilic muscle fibres, with nuclear ghosts, areas of extensive degeneration, disappearance of muscle architecture with sarcoplasmic vacuolation, thick walled arteries, and congested veins (Fig. 2 b & c).
- Group III showed degenerated pale acidophilic muscle fibres, with nuclear ghosts, areas of extensive degeneration, disappearance of muscle architecture with mononuclear cell infiltration, with extremely pyknotic nuclei (Fig. 2 d & e).
- Group IV showed apparently normal architecture of parallel skeletal muscle fibres with acidophilic striated sarcoplasm and peripheral oval vesicular nuclei. Loose connective tissue endomysium separating the muscle fibres (Fig. 2 f) (Fig. 2).

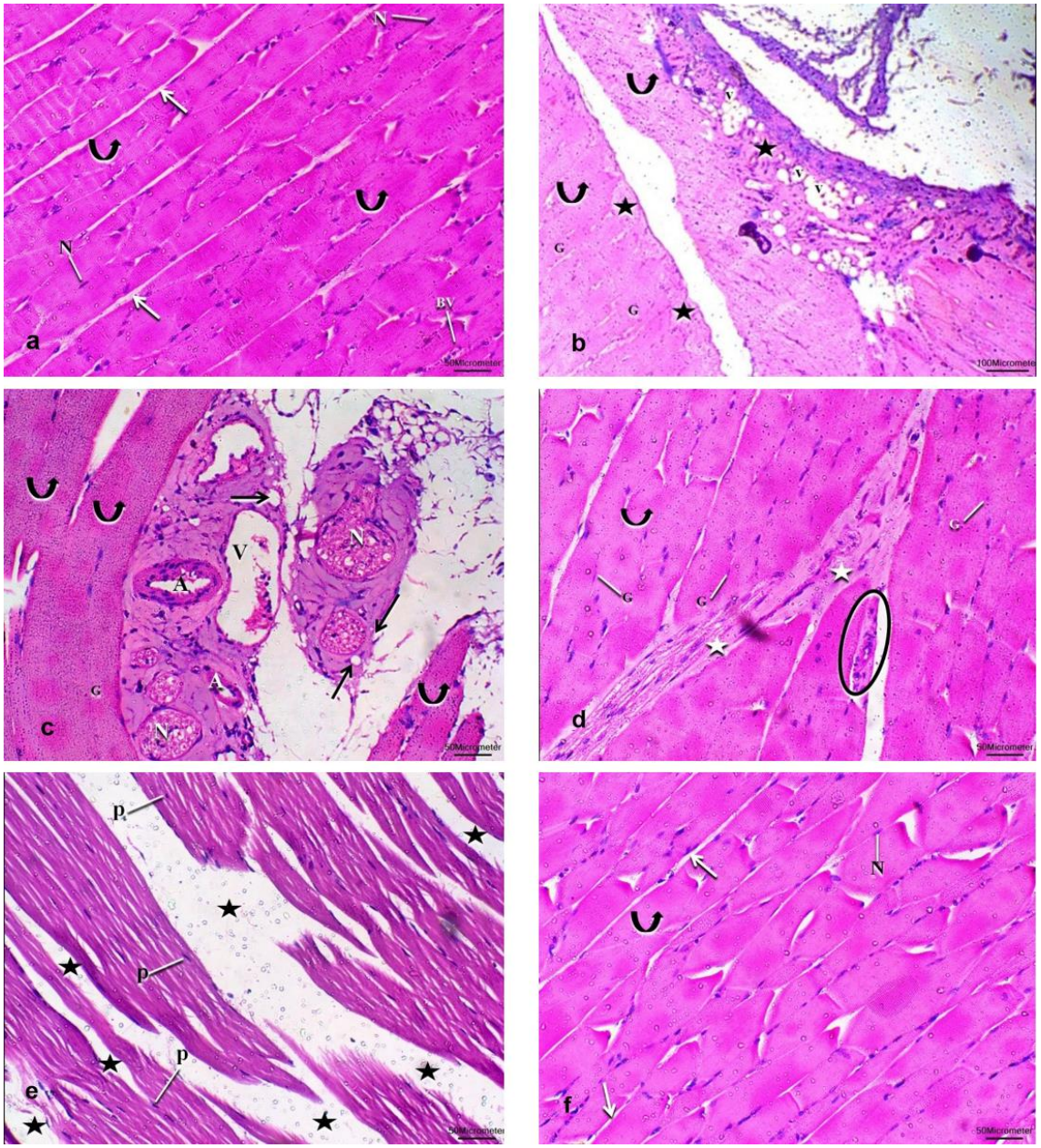

Fig. 2: Photomicrographs of H&E stained sections of rat skeletal muscles: a) (group I) showing normal architecture of skeletal muscle with parallel muscle fibres, acidophilic striated sarcoplasm (curved arrow) and peripheral oval vesicular nuclei (N). Loose connective tissue endomysium separating the muscle fibres(thin arrow) and featuring a small blood vessel (BV).b) & c) (group II) showing degenerated pale acidophilic muscle fibres (curved arrows), with nuclear ghosts (G), loss of muscle architecture (star) with sarcoplasmic vacuolation (v) and (thin arrows), thick walled arteries (A), congested veins (V). d) & e) (group III) showing degenerated pale acidophilic muscle fibers (curved arrows), with nuclear ghosts (G), loss of muscle architecture (star) with mononuclear cell infiltration (circle) and extremely pyknotic nuclei(p).f) (group IV) showing apparently normal architecture of muscle fibres with acidophilic striated sarcoplasm (curved arrow) and peripheral oval vesicular nuclei (N). Loose connective tissue endomysium separates the muscle fibres (thin arrow). (Hx & E x 200)

Masson's trichrome stain results:

Collagen fibres deposition between muscle fibres and around blood vessels was normal in group I (Fig. 3 a), massive in Group II (Fig. 3 b), moderate in group III (Fig.3 c), and minimal in group IV (Fig. 3 d) (Fig. 3).

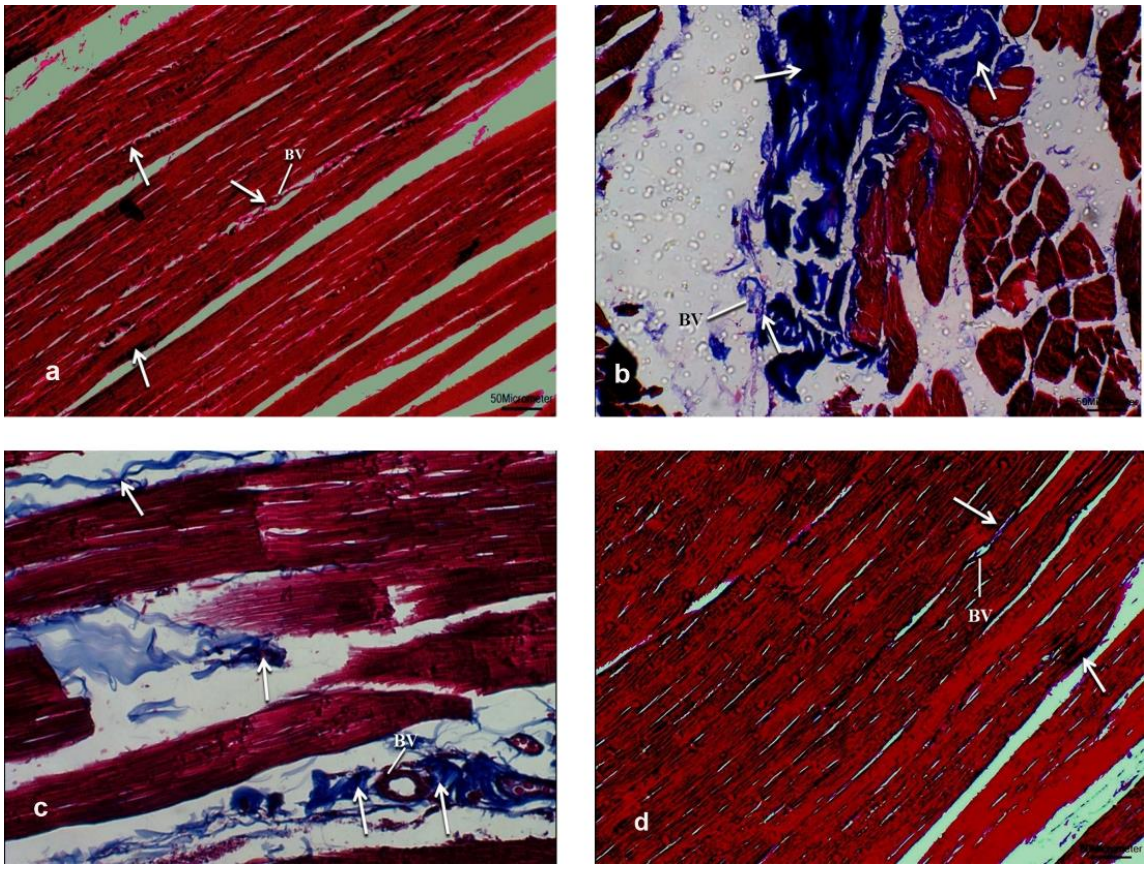

Fig. 3: Photomicrographs of a Masson stained sections of rat skeletal muscles: a) (group I) showing normal collagen fibres deposition (arrow) between muscle fibres and around blood vessels(BV). b) (group II) showing massive increase of collagen fibres deposition (arrow) between muscle fibres and around blood vessels(BV). c) (group III) showing moderate increase of collagen fibres deposition (arrow) between muscle fibres and around blood vessels(BV). d) (group IV) showing minimal collagen fibres deposition (arrow) between muscle fibers and around blood vessels(BV). (Masson's trichrome x 200)

Electron microscopic results:

- Group I: EM examination revealed myofibrils with peripheral oval nuclei. The adjoining longitudinal section of muscle fibre exhibited normal peripheral nucleus with euchromatin and peripherally condensed heterochromatin and mitochondria with normal cristae pattern. Alternating dark bands and light bands with regular Z lines inside and sarcomere between 2 successive lines. Each myofibril was separated from each other by a space containing mitochondria, glycogen rosettes and smooth endoplasmic reticulum cisterns (Fig. 4 a&b).
- Group II: EM examination revealed nuclei with peripheral condensation of chromatin clumps, absent myofibrils, interrupted myofibrils, dilated cisterns of smooth endoplasmic reticulum and ballooned mitochondria with damaged cristae (Fig. 4 c & d).
- Group III: EM examination revealed extensively absent myofibrils that replaced in some areas by dense granules, dilated cisterns of smooth endoplasmic reticulum and ballooned mitochondria with damaged cristae (Fig. 4 e).
- Group IV: EM examination revealed alternating dark bands and light bands with regular Z lines inside parallel myofibrils. Myofibrils were separated from each other by a space containing apparently normal mitochondria, and smooth endoplasmic reticulum cisterns (Fig. 4 f) (Fig. 4).

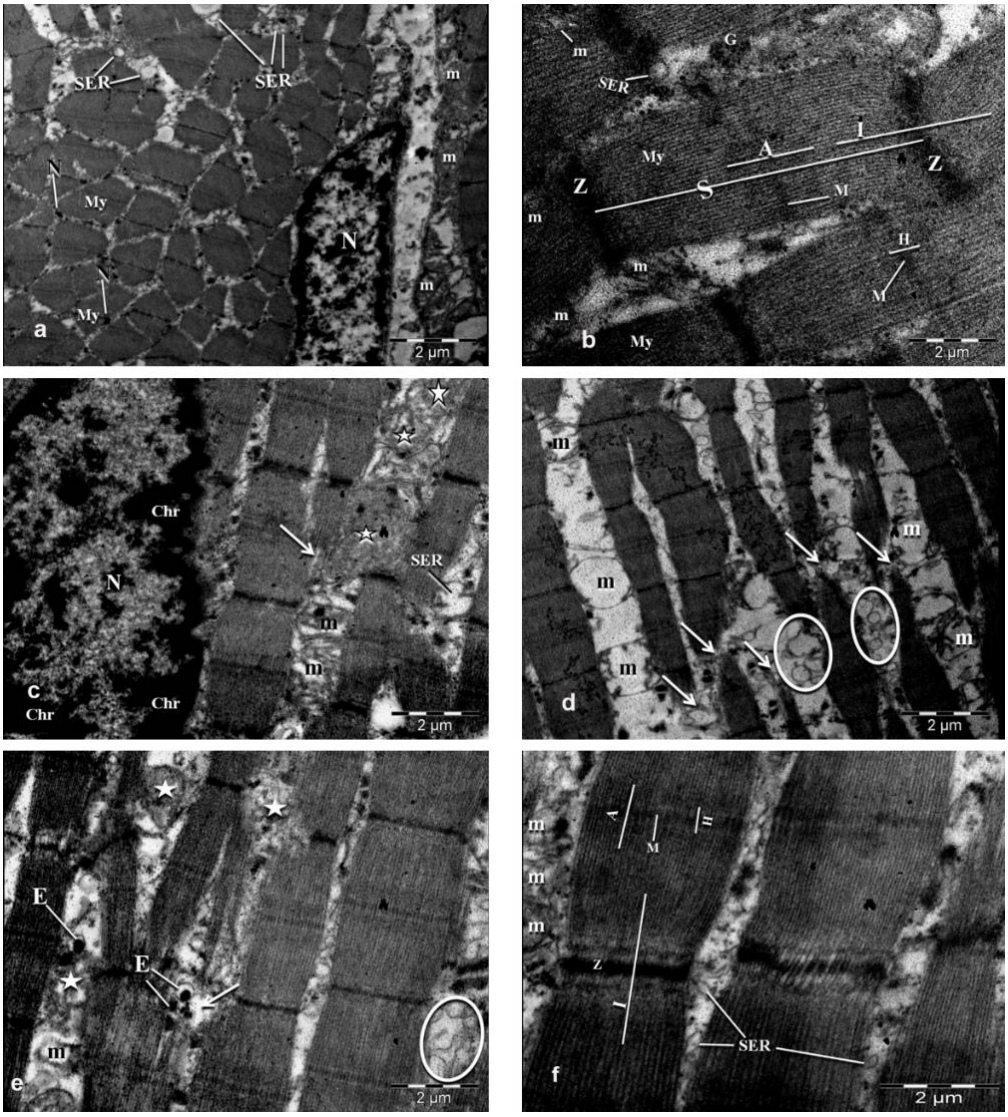

Fig. 4: Electron micrographs of a section of rat skeletal muscles: a) (group I) showing myofibrils (My) with peripheral oval nuclei (N) with smooth endoplasmic reticulum Cisterns (SER) in-between. The longitudinal section of muscle fiber exhibits normal peripheral nucleus (N) with euchromatin and peripherally condensed heterochromatin and mitochondria normal cristae pattern (m). b) (group I) showing eucheomatic nucleus (N), alternating dark bands (A) and light bands (I) with regular Z lines and sarcomere (S) between 2 successive (Z) lines, parallel myofibrils (My). Myofibrils are separated by a space containing mitochondria (m), glycogen rosettes (G) and smooth endoplasmic reticulum cisterns (SER). c) & d) (group II) showing a nucleus (N) with peripheral condensation of chromatin clumps (Chr), absent myofibrils(star), interrupted myofibrils (arrow), dilated cisterns of smooth endoplasmic reticulum (SER) and (Circles) and ballooned mitochondria with damaged cristae (m). e) (group III) showing absent myofibrils (star) replaced by dense granules (E), dilated cisterns of smooth endoplasmic reticulum (Circle) and ballooned mitochondria with damaged cristae (m). f) (group IV) showing alternating dark bands (A) and light bands (I) with regular Z lines inside parallel myofibrils. Myofibrils are separated by a space containing apparently normal mitochondria (m), and smooth endoplasmic reticulum cisterns (SER). (TEM a) x 15000 & b) x 28000, c) & e) x 24000, d) x 20000, f) x 28000)

Collagen area percent:

It was significantly higher in group II and group III when compared to control group. There was non significant difference between group I and IV, although, it showed a significantly lower level in group IV when compared to group II and III (Fig. 5).

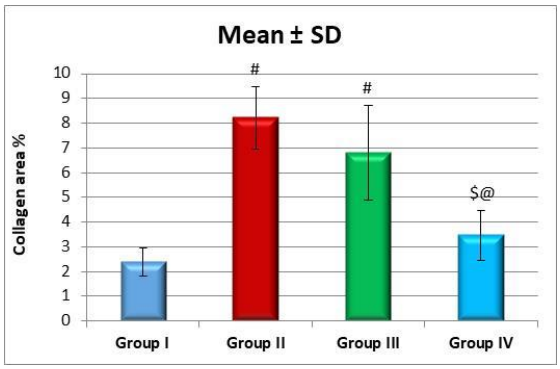

Fig. 5: Collagen area percent in the skeletal muscle fibres among different groups of the investigated animals
significant from control, $ significant from group II, @ significant from group III

Antioxidant Enzymes activity:

There was no statistically significant difference in SOD and Catalase levels among group I and IV. There was non significant difference between group II and group III. However, SOD and catalase levels were statistically higher in group IV when compared to group II and III which prove the regeneration and survival capability of MSCs (Figure 6, 7).

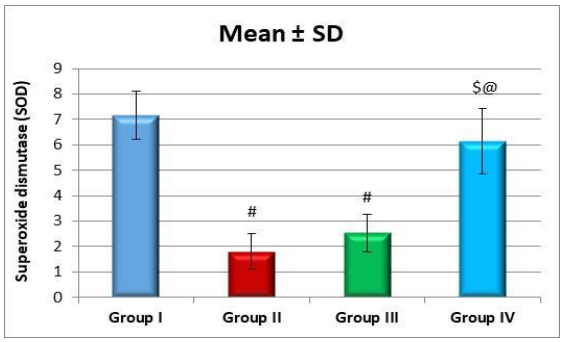

Fig.6: SOD Levels among different groups of the investigated animals
significant from control, $ significant from group II, @ significant from group III

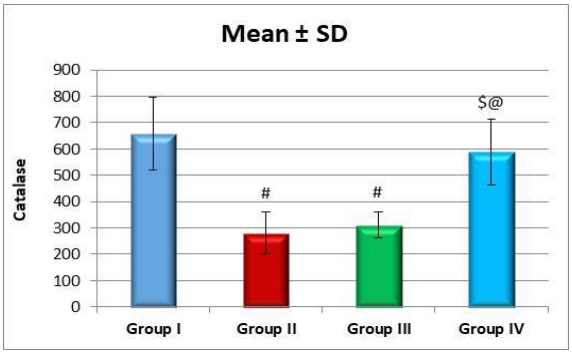

Fig.7: Catalase levels among different groups of the investigated animals
significant from control, $ significant from group II, @ significant from group III

DISCUSSION

MSCs have extended traction in treatment of various degenerative and immune disorders [34, 35]. In the present study, we investigated the therapeutic efficacy of MSCs and the diagnostic value of TNF-α and IL-1β in doxorubicin-induced skeletal myopathy.

Our study proved that rats treated with systemic MSCs showed obvious signs of skeletal muscle regeneration demonstrated by significant alteration in the histological and laboratory results. In that group, skeletal muscle fibres showed apparently normal architecture.

Although, the present work demonstrated that skeletal muscles specimens of the group of rats left for spontaneous recovery showed areas of extensive degeneration, and disappearance of muscle architecture.

This could be explained by the fact that the skeletal muscles regeneration is mediated by resident satellite cells, both of hematopoietic and mesenchymal origin. Initially, BM derived cells settle in the perivascular interstitial tissue and display relatively low myogenic potential. Therefore, the muscle tissue has poor spontaneous regeneration [13, 34].

Burdzińska, et al. [14] reported that muscle injury initiates mobilization of BMMSCs from bone marrow to the peripheral blood. These MSCs reside in skeletal muscle then differentiate into mature myocytes through Bystander effect which is induced by factors secreted by SCs.

Wang et al.[35] stated that release of vascular endothelial growth factor from SCs improves the blood supply and enhances tissue regeneration. Similarly, we demonstrated higher levels of VEGF gene expression in SCs treated group.

The present study elucidated an antioxidant capability of MSCs in the treated group in terms of significantly high levels of SOD and catalase enzymes. These findings proved the crucial post-transplantation and survival advantage of MSCs. Previous studies demonstrated that MSCs administration had antioxidant effect on skeletal muscles by inducing high levels of SOD and glutathione [36] .

Conversely, another study reported that infused umbilical cord stem cells exert profibrogenic potential in treatment of hepatic injury [37]. This could be explained by the fact that stem cell could be a double edge sward therapy depending on the route of transplantation [38].

Inflammatory cytokines have a crucial role in regulating tissue damage and regeneration. One of the suggested attributors to muscle dysfunction in doxorubicin- treated patients, is its ability to elevate serum TNF-α levels [7].

TNF is produced by a variety of cells, including cardiac and skeletal myocytes [39].

TNF induces contractile dysfunction through binding to TNF-receptors in the skeletal myofibrils [7, 36].

In the present study, two inflammatory mediators, TNF-α and IL-1β have been investigated as potential indicators for evaluation of the therapeutic efficiency of MSC for doxorubicin- induced skeletal myopathy. Analysis of our findings revealed noteworthy lower levels of both TNF-α and IL-1β in MSCs treated group. In agreement, other studies demonstrated the ability of SCs to lessen TNF-α, IL-1β levels thereby ameliorating tissue injury [12, 36].

CONCLUSION

MSCs is a promising therapy for doxorubicin-induced skeletal myopathy. TNF-α and IL-1β are helpful biomarkers for evaluation of SCs therapeutic efficacy.

Previous publication or presentation: No
Source of funding: No funding

Conflicts of interest:
The authors declare that they have no financial or non financial conflicts of interest related to the work done in the manuscript.

- Each author listed in the manuscript had seen and approved the submission of this version of the manuscript and takes full responsibility for it.
- This article had not been published anywhere and is not currently under consideration by another journal or a publisher.

REFERENCES

1. Carvalho C, Santos R, Cardoso S, Correia S, Oliveira PJ, Santos MS, Moreira PI. Doxorubicin: The good, the bad and the ugly effect. Curr Med Chemist., 2009; 16 (25), 3267-85.
2. Arcamone F, Cassinelli G, Fantini G, Grein A, Orezzi P, Pol C. Adriamycin, 14-hydroxydaunomycin, a new antitumor antibiotic from S. peucetius var. caesius.
   Bio technol Bioeng., 1967; 11:1101– 010
3. Di Marco A, Gaetani M, Scarpinato B. Adriamycin (NSC-123,127): a new antibiotic with antitumor activity. Cancer Chemother Rep., 1969;53:33–37
4. Min K, Kwon OS, Smuder A J, Wiggs M P, Sollanek K J, Christou D.D, Yoo J K, Hwang M H, Szeto H. Increased mitochondrial emission of reactive oxygen species and calpain activation are required for doxorubicin-induced cardiac and skeletal muscle myopathy. The Journal of Physiology, 2015; 593(8): 2017–2036.
5. Thorn CF, Oshiro C, Marsh S, Hernandez-Boussard T, McLeod H, Klein TE. Doxorubicin pathways: Pharmacodynamics and adverse effects. Pharmacogenetics and Genomics, 2011; 21(7): 440-446.
6. Adams V, Mangner N, Gasch A, Krohne C, Gielen S, Hirner S, Thierse HJ, Witt CC. Induction of MuRF1 is essential for TNF-alpha-induced loss of muscle function in mice. J Mol Biol., 2008; 384: 48–59, 2008
7. Gilliam L A, Clair D KS, Reid M B. Doxorubicin acts through tumor necrosis factor receptor subtype 1 to cause dysfunction of murine skeletal muscle. J. Appl. Physiol., 2009; 107: 1935–1942.
8. Salles G, Bienvenu J, Bastion Y, Barbier Y, Doche C, Warzocha K, Gutowski MC, Rieux C. Elevated circulating levels of TNF-α and its p55 soluble receptor are associated with an adverse prognosis in lymphoma patients. Br J Haematol., 1996; 93: 352–359.
9. Tangpong J, Cole MP, Sultana R, Joshi G, Estus S, Vore M, St CW, Ratanachaiyavong S. Adriamycin-induced, TNF-alpha-mediated central nervous system toxicity. Neurobiol Dis., 2006; 23: 127–139.
10. Feng SW, Lu X L, Liu Z S, Zhang Y N, Liu TY, Li JL. Dynamic distribution of bone marrow-derived mesenchymal stromal cells and change of pathology after infusing into mdx mice. Cytotherapy, 2008; 10:254-264.
11. Singh A, Singh A, Sen D. Mesenchymal stem cells in cardiac regeneration: a detailed progress report of the last 6 years (2010-2015).Stem Cell Res. Ther., 2016; 7 (1):82.
12. Zaghloul S S, Abo-El nour R K, Abdel Fattah M M, Ismail DI. Comparative Histological Study on the Effect of Mesenchymal Stem Cell and Losartan on Cardiac Injury Induced by Doxorubicin in Male Albino Rats. Egyptian Journal of Histology, 2020; 42(4): 815 825.
13. Guis S, Figarella-Branger D, Mattei J P, Nicoli F, Kozak-Ribbens G. Association between statin-associated myopathy and skeletal muscle damage. CMA., 2009; 181: 8-11
14. Burdzińska A, Gala K, Paczek L. Myogenic stem cells. Folia Histochem. Cytobiol., 2008; 46:401-412.
15. Drapeau C, Antarr D, Ma H, Yang Z, Tang L, Hoffman RM. Mobilization of bone marrow stem cells with Stem Enhancer improves muscle regeneration in cardiotoxin-induced muscle injury. Cell Cycle, 2010; 9:1819-23.
16. Alhadlaq A, Mao JJ. Mesenchymal stem cells isolation and therapeutics. Stem cells Dev. 2004; 13: 436-48.
17. Payushina OV, Domaratskaya EI, Starostin VI. Mesenchymal Stem Cells: Sources, Phenotype, and

Differentiation Potential. Biology Bulletin, 2006; 33, 1:2-18.

18. Kyriakou C, Rabin N, Pizzey A, Nathwani A, Yong K. Factors that influence short-term homing of human bone marrow-derived mesenchymal stem cells in a xenogeneic animal model. Haematologica, 2008; 93: 1457-65.
19. Louis KS, Siegel AC. Cell viability analysis using trypan blue: manual and automated methods. Methods Mol. Biol., 2011; 740: 7-12
20. Zhang X J, Cao XQ, Zhang CS, Zhao Z. 17β-estradiol protects against doxorubicin-induced cardiotoxicity in male Sprague-Dawley rats by regulating NADPH oxidase and apoptosis genes. Molecular Medicine Reports, 2017; 15, 5: 2695–702
21. Levicar N, Pai M, Habi NA, Tait P Jiao, Marley LR, Davis SB, Dazi J, Gordon M Y. Long-term clinical results of autologous infusion of mobilized adult bone marrow derived CD34 cells in patients with chronic liver disease. Cell prolif., 2008; 41:115-125.
22. Yang L, Liu G, Zhu X, Luo Y, Gu XL.The anti-inflammatory and antioxidant effects of leonurine hydrochloride after lipopolysaccharide challenge in broiler chicks. Poultry Science, 2019; 98:1648–1657.
23. Winer J, Jung CK, Shackel I, Williams PM. Development and validation of real-time quantitative reverse transcriptase-polymerase chain reaction for monitoring gene expression in cardiac myocytes in vitro. Anal Biochem., 1999; 270:41±49.
24. Chang CW, Christensena LV, Leeb M, Kima SW. Efficient Expression of Vascular Endothelial Growth Factor Using Minicircle DNA for Angiogenic Gene Therapy. J. Control Release, 2008; 125(2): 155–163.
25. Kiernan JA. Histological and histochemical methods: theory and practice, 5th edition, 2015; Scion publishing ltd. Vantage business park, Boxham road, Banhury, UK.
26. Calvi ENV, Nahas FX, Barbosa MV, Calil JA. Ferreira LM. An experimental model for the study of collagen fibers in skeletal muscle. Acta Cirúrgica Brasileira, 2012; 27 (10): 681- 686.
27. Hayat MA. Principles and techniques of electron microscopy: Biological applications, 4th ed., 2000; Cambridge: Cambridge University Press.
28. Hadlock TA, Kim SW, Knox CJ, Weinberg J, Heaton JT. Quantitative Histologic Analysis of Muscle Micro-architecture Following Facial Nerve Injury in a Rodent Model. JAMA Facial Plast. Surg., 2013; 15(2): 141–146.
29. Sullivan-Gunn MJ, Lewandowski PA. Elevated hydrogen peroxide and decreased catalase and glutathione peroxidase protection are associated with aging sarcopenia. BMC Geriatrics, 2013; 13:104.
30. Alves Pereira LM, Monteiro I C G, Dos- Santos L HP, Ferraz M, Loureiro A C, Lima CC, Ceccatto VM. Strenuous Acute Exercise Induces Slow and Fast Twitch-Dependent NADPH Oxidase Expression in Rat Skeletal Muscle. Antioxidants, 2020; 9:57
31. Armitage P, Berry G. Statistical methods in medical research, 3rd ed., Blackwell Scientific Publications, London, 1994.
32. Brennen WN, Denmeade SR, Isaacs JT. Mesenchymal stem cells as a vector for the inflammatory prostate microenvironment. Endocr Relat Cancer, 2013; 20: R269–290.
33. Yehia H, Elshimy A, ElZainy A , Dina Fawzy D. Evaluation of Mesenchymal Stem cells as an Adjuvant Therapy in Treatment of Induced Experimental Autoimmune Prostatitis in Albino Rats. EJMM, 2019; 28: 3
34. Martin CM, Hawke TJ, Garry DJ. Stem Cells and Muscle Regeneration. In: Principles of Molecular Medicine. 2rd ed. Runge MS, Patterson C, Eds. Humana Press Inc: Totowa N.J., 2006; 12: 682-687.
35. Wang M, Tsai BM, Crisostomo PR, Meldrum DR. Pre-treatment with adult progenitor cells improves recovery and decreases native myocardial proinflammatory signaling after ischemia. Shock, 2006; 25: 454–459.
36. Urish KL, Vella jb, Okada M, Keller B B, Huard J. Antioxidant Levels Represent a Major Determinant in the Regenerative Capacity of Muscle Stem Cells. Mol Biol Cell, 2009; 20 (1): 509-020
37. Di Bonzo LV, Ferrero I, Cravanzola C. Human mesenchymal stem cells as a two-edge sword in hepatic regenerative medicine: engraftment and hepatocyte differentiation versus profibrogenic potential. Gut, 2008; 57: 223-231.
38. Idriss NK, Sayyed HG, Osama A, Sabry D. Treatment Efficiency of Different Routes of Bone Marrow-Derived Mesenchymal Stem Cell Injection in Rat Liver Fibrosis Model Cellular Physiology and Biochemistry, 2018; 48:2161-2171.
39. Gielem S, Adams V, Mobius-Winkler S, Schuler G, Hambrecht R. Anti-inflammatory effects of exercise training in the skeletal muscle of patients with chronic heart failure. J Am Coll Cardiol., 2018; 42: 861–868, 2003